



Title	Diversity of clustered protocadherin- α genes in neuronal identity and its role in short-term specific associative memory formation
Author(s)	大須賀, 智輝
Citation	大阪大学, 2025, 博士論文
Version Type	VoR
URL	https://doi.org/10.18910/103170
rights	
Note	

The University of Osaka Institutional Knowledge Archive : OUKA

<https://ir.library.osaka-u.ac.jp/>

The University of Osaka

**Diversity of *clustered protocadherin- α* genes in neuronal identity and its
role in short-term specific associative memory formation**

クラスター型プロトカドヘリン α の多様性が短期記憶特異的な神経回路形成に果たす役割

大阪大学大学院 生命機能研究科

大須賀 智輝

令和 7 年 9 月修了

Abstract

Clustered protocadherins (cPcdh) are a family of cell adhesion molecules that contribute to synaptic specificity and neuronal connectivity and have been implicated in cognitive function. *cPcdh* comprises 58 isoforms, classified into three subgroups: *cPcdh- α* , *cPcdh- β* , and *cPcdh- γ* . The expression patterns of these isoforms suggest a role in neural circuit organization, although their precise functions remain unclear. In this study, I investigated how reduced *cPcdh* α diversity affects memory function using *cPcdh α 1-12* mutant mice, which express only two variable α -isoforms. Memory function was analyzed separately for short-term and long-term memory using a modified Context Pre-exposure Facilitation Effect (CPFE) paradigm, with intervals of 2 h for short-term memory and 24 h for long-term memory. Behavioral analyses revealed that *cPcdh α 1-12* mice exhibited significant impairments in short-term memory, failing to discriminate the conditioned context from a novel context at the 2 h interval, while their long-term memory at the 24 h interval remained intact. In contrast, *cPcdh α 1-12* mice showed no abnormalities in spontaneous locomotion or general exploratory behavior, indicating that their impairment was specific to short-term memory rather than a general deficit in motor function or learning ability. Furthermore, analysis of neural activity during memory recall revealed significantly reduced activation in the hippocampus, amygdala, and retrosplenial cortex in *cPcdh α 1-12* mice during short-term memory tasks, suggesting reduced engagement of these circuits in

memory encoding. Finally, based on these findings, we examined whether similar regions were involved in short-term memory recall in wild-type mice. Analysis in wild-type mice showed that these same regions, including CA3, basolateral amygdala, and retrosplenial cortex, exhibited increased neural activity during short-term memory recall, whereas long-term memory recall did not show such activation patterns. These findings suggest that short-term and long-term memory relies on distinct neural circuits and that *cPcdh* α diversity is essential for the formation and function of circuits required for short-term memory. This study provides insights into the molecular and neural mechanisms underlying memory and highlights the importance of *cPcdh* α diversity in maintaining short-term memory processes.

INDEX

Contents	Page
General introduction	1
Introduction	6
Results	8
Discussion	24
Material and methods	30
References	37
Acknowledgments	46
Accomplishments	47

General introduction

Memory is a fundamental process that enables the storage and retrieval of experiences and information as needed, forming the core of cognitive function. The brain retains this information through complex neural networks, allowing us to recall past experiences, learn new skills, and adapt to changing environments. Studies have demonstrated that memory is not confined to a single region of the brain but is distributed across functionally interconnected areas, such as the hippocampus¹⁻⁶, amygdala⁷⁻¹⁴, and cortex¹⁵. This distribution presents significant challenges in comprehensively explaining the mechanisms underlying the formation of specific types of memory. Furthermore, memory undergoes a transformation from a transient and unstable state immediately after an experience to a stable, long-term state through a series of molecular and cellular processes.

In the case of fear memory, the recall process mediated by the basolateral amygdala (BLA) has been shown to involve hippocampus-dependent pathways for short-term memory and prefrontal cortex-dependent pathways for long-term memory¹⁶. This suggests that the transition from short-term to long-term memory occurs through functional reorganization of neural circuits. The processes of memory consolidation and stabilization are thought to involve changes occurring over seconds, days, months, and even years²⁰. These processes include synaptic plasticity, reorganization of neuronal connections, and the formation of new synapses, all of which rely on

temporally and spatially precise molecular mechanisms.^{2,16-19} Findings from systems-level and molecular studies have indicated that memory retrieval within a few hours of learning, as opposed to after 24 h, may rely on distinct mechanisms across brain regions. Both pharmacological and genetic experimental evidence supports the view that memory retrieval around 1–3 h after learning is mechanistically distinct from retrieval at 24 h or later. Pharmacological blockades of specific hippocampal receptors impair memory at 1.5 hours, but not at 24 h²¹. Knockout mice lacking PKC- γ exhibit selective memory retention deficits between 10 min and 3 h, while long-term memory remains intact²². While these observations support the concept of a functional distinction between short-term and long-term memory, the underlying biological mechanisms are not well understood. Understanding this distinction is essential for discovering how memory traces evolve over time and across neural circuits. In recent studies, advanced tools such as viral tracer technologies and optogenetics-based manipulation of neuronal ensembles have provided powerful means to elucidate these mechanisms. However, precisely identifying these processes across multiple brain regions and over extended time periods remains an exceptionally challenging task.

In this study, I utilized a transgenic mouse model with genetic abnormalities specifically affecting short-term memory formation to investigate these processes. Clustered protocadherins (*cPcdhs*) are genes known to regulate synaptic specificity through their highly diversified variable

region exons. Previous studies have demonstrated that transgenic mice with reduced diversity in *cPcdh* expression exhibit specific deficits in short-term memory formation. Interestingly, however, these mice showed no abnormalities in long-term memory tasks, such as 24 h and 2 weeks fear conditioning, compared to wild-type mice. These findings challenge the conventional view that short-term memory and long-term memory are continuous processes and that intact short-term memory is a prerequisite for long-term memory formation, as suggested by previous studies^{23,24}. I aim to conduct a detailed analysis of this transgenic mouse model, which exhibits abnormalities specifically in short-term memory, to gain new insights into the processes of memory stabilization and consolidation. Furthermore, I anticipate that our findings will provide critical evidence demonstrating that proper neural circuit formation mediated by clustered protocadherins (*cPcdhs*) is essential for higher-order cognitive functions that enable short-term memory.

Clustered Protocadherin

In this study, I focused on clustered protocadherins (*cPcdhs*), membrane proteins with specific cell adhesion activity. *cPcdhs* consist of three gene clusters, α , β , and γ , comprising 14, 22, and 22 isoforms, respectively, and are predominantly expressed in neuronal cells²⁵⁻²⁸. Each isoform is preceded by a promoter region, enabling the expression of diverse combinations of *cPcdhs* through random selection of variable regions in individual neurons. This mechanism

imparts cell specificity²⁹⁻³¹. Intriguingly, *cPcdh* proteins form *cis*-dimers and exhibit highly specific trans-homophilic adhesion activity through their extracellular domains³². In vitro studies have demonstrated that when five *cPcdh* isoforms are expressed, cell aggregation does not occur unless at least one isoform is identical between cells. This finding highlights the exceptionally high specificity of *cPcdh*-mediated adhesive activity³³.

Clustered Protocadherin alpha

The mouse *Pcdhα* gene cluster comprises 14 variable exons ($\alpha 1-\alpha 12$, $\alpha c1$, $\alpha c2$). Each variable exon is transcribed from its own unique promoter and spliced to the constant region exons (CR1–CR3), which are shared by all *Pcdhα* genes. The expression of *Pcdhα* transcripts is governed by the genomic structure of the *Pcdhα* gene cluster, which plays a crucial role in determining the stochastic and constitutive expression patterns of variable exons. Alterations in the number or arrangement of variable exons within the cluster impact expression frequencies, yet the total expression level of *Pcdhα* transcripts remains stable, maintained by robust *cis*-regulatory mechanisms³⁴. These findings underscore the role of genomic architecture in *Pcdhα* regulation and suggest that structural variations may impact neural circuit formation and DNA methylation.

Context Pre-exposure Facilitation Effect (CPFE)

The Context Pre-exposure Facilitation Effect (CPFE) is a fear conditioning paradigm which separates the acquisition of contextual information from its association with an aversive stimulus³⁵. In this procedure, animals are first exposed to a novel context without any reinforcement. On a subsequent day, they receive an immediate foot shock upon re-entering the same context. Under typical conditions, an immediate shock does not facilitate contextual fear learning due to the insufficient time available for context encoding. However, when pre-exposure occurs, robust contextual fear responses are observed, indicating that the earlier acquired context representation can be retrieved and associated with shock. CPFE thus provides a useful framework for investigating how contextual and aversive memories are encoded independently and integrated over time.

Introduction

The brain is an extremely complex system that processes vast amounts of information, relying on the specific connections and coordinated interactions of billions of neurons for functions such as sensory integration, memory formation, and cognition. The precise formation of these neural circuits is essential for proper brain function, and disruptions in this process can lead to significant cognitive and behavioral impairments³⁶.

Clustered protocadherins (*cPcdh*) are cell adhesion molecules that mediate neuronal connections and are essential for synaptic specificity and neural circuit formation^{25,37}. *cPcdh* comprise 58 isoforms, categorized into three subgroups: *cPcdh α*, *cPcdh-β*, and *cPcdh-γ*²⁶. Each neuron expresses these isoforms in diverse combinations, forming specific synaptic connections through interactions between identical isoforms³⁸⁻⁴¹. This molecular diversity is thought to be critical for the formation of neural circuits, which are essential for higher brain functions such as memory and cognition^{42,43}. Thus, unraveling the complexity of neural circuit formation requires clarifying the role of *cPcdh* in synapse formation, an important topic in neuroscience. Although it is known that *cPcdh* contribute to synaptic specificity, the functional impact of reduced *cPcdh* isoform diversity on neural circuits and behavior has not been fully elucidated. To investigate the functional significance of *cPcdh* diversity, a genetically modified mouse model called *cPcdh α1-12* mice has been developed. In this model, only *cPcdh-α1* and *α12* of the 12 variable isoforms

are expressed, while two α C1 and α C2 constant isoforms are also retained^{31,34,44}. The *cPcdh- α 1-12* mice exhibit a phenotype similar to that of wild-type mice in appearance and general behavior, but they display deficits in certain higher brain functions, particularly in sensory integration, short-term visual memory, and audiovisual associative memory^{45,46}. These impairments are evident in poorer task performance, emphasizing the critical role of *cPcdh- α* isoform diversity in neural circuit formation and higher brain functions. Despite these observations, the neural mechanisms responsible for these deficits remain to be elucidated, highlighting the need for further investigation into the molecular and circuit-level changes in *cPcdh- α 1-12* mice.

The aim of this study is to investigate the effects of reduced *cPcdh- α* diversity on the behavior and cognitive function of *cPcdh- α 1-12* mice by first conducting multiple behavioral experiments to comprehensively evaluate their cognitive functions. In addition, changes in neural activity will be observed simultaneously using neuronal activity markers to examine the relationship between cognitive impairments and alterations in neural activity. We hypothesize that reduced *cPcdh- α* diversity causes behavioral deficits and changes in neural activity, providing new insights into the molecular mechanisms related to neural circuit formation and cognitive functions.

Result

Assessment of behavioral traits in *cPcdh α1-12* mice lacking protocadherin diversity

In this study, I assessed the behavioral traits and activity levels of *cPcdh α1-12* mice in which α2 to α11 of the 12 clustered protocadherin α isoforms are deleted (Fig. 1a). Activity in the home cage was monitored over 24 h using nanotags and showed no significant differences in activity levels between *cPcdh α1-12* mice and wild-type mice (Fig. 1b). In addition, an open-field test was performed to assess locomotor activity and anxiety-like behavior. The results showed no significant differences between the two groups in distance traveled at 5 min intervals (Fig. 1c), total distance traveled (Fig. 1d), and time spent in the central area (Fig. 1e).

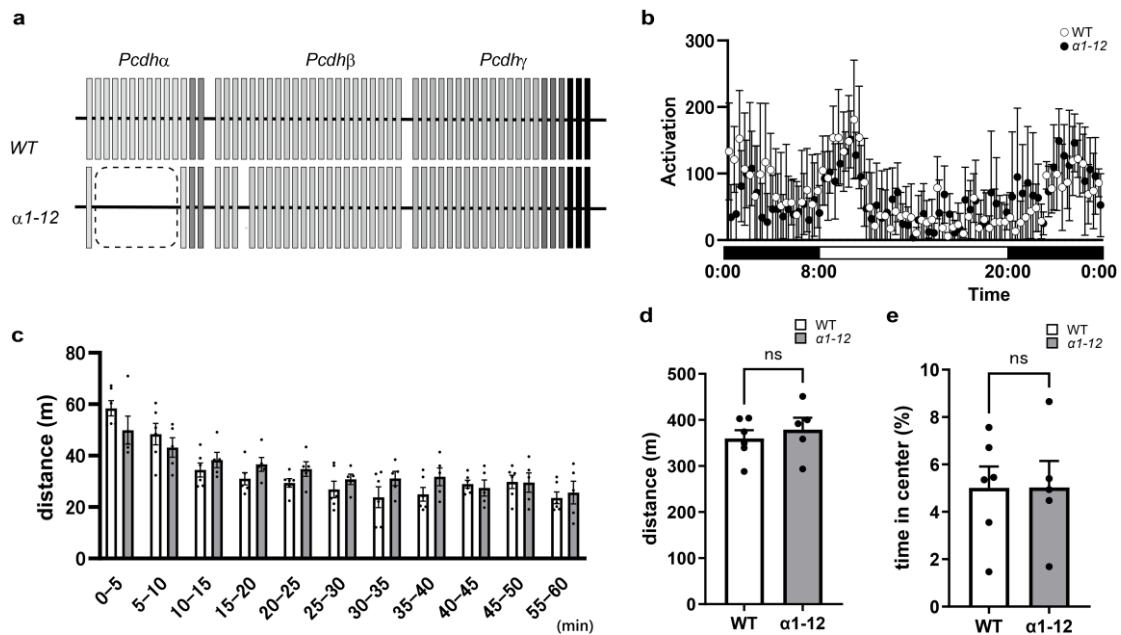


Figure 1 Behavioral assessment and activity monitoring in *cPcdh* α 1-12 mice

(a) Schematic of *cPcdh* α 1-12 mice, showing the deletion of *cPcdh* α 2 to α 11. (b) Home cage activity monitored over 24 h using nanotags. No significant differences in activity levels were detected between the two groups. (c, d, e) Open field test results: (c) distance traveled in 5 min intervals, (d) total distance traveled, (e) time in the central area. No significant differences between wild-type (n=6, male 3, female 3) and *cPcdh* α 1-12 (n=5, male 3, female 2).

Short-term memory deficits in *cPcdh α1-12* mice

Previous studies have suggested that *cPcdh α1-12* mice may have specific deficits in short-term memory compared to wild-type mice, as assessed by the T-maze task, which consists of visually guided and memory-guided tasks⁴⁶. However, in previous studies, mice took over a minute to reach their destination, leading to significant variability between trials and making it difficult to accurately measure memory retention time. To address this problem, I minimized stress on the mice and retested the experiment under improved conditions. First, the mice were trained in a visually guided task (Fig. 2a). Wild-type mice learned to select the correct arm marked by a visual cue to receive a reward, and both *cPcdh α1-12* and wild-type mice showed similar performance, reaching stable scores within 15 days. Once mice achieved a success rate of 80% or more higher on three separate days, they transitioned to the memory-guided task, where visual cues were replaced with memory-based cues, requiring them to rely on short-term memory to select the correct arm. Following the transition to the memory-guided task, which required short-term memory, the performance of wild-type mice was initially suppressed to chance levels immediately after a task switch and gradually recovered to the performance level before the switch (Fig. 2b). In contrast, *cPcdh α1-12* mice showed a similar initial suppression after the task switch, but no subsequent recovery was observed. As a result, the performance of *cPcdh α1-12* mice was significantly lower than that of wild-type mice (Fig. 2c). In addition, the time required

for choice selection was significantly reduced compared to previous studies, confirming that *cPcdh α1-12* mice exhibit abnormalities in the formation of short-term memory lasting only a few seconds compared to wild-type mice (Fig. 2d).

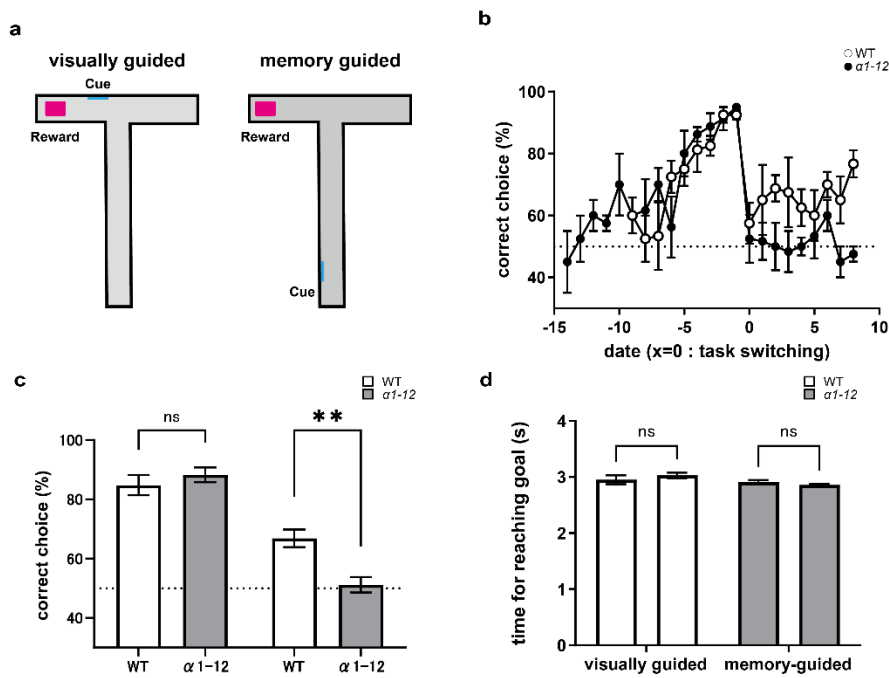


Figure 2 T-maze performance in *cPcdh* $\alpha 1-12$ and wild-type mice

(a) Schematic diagram of the T-maze task. Left panel illustrates the visually guided task and right panel illustrates the memory-guided task. (b) After task switching ($x = 0$), wild-type mice initially showed a decline in performance in both visually-guided and memory-guided tasks but subsequently recovered. In contrast, *cPcdh* $\alpha 1-12$ mice showed a decline specifically in the memory-guided task without recovery (wild-type $n=4$, male 2, female 2; *cPcdh* $\alpha 1-12$ $n=4$, male 2, female 2). (c) Mean performance in the last five sessions (100 trials). There was no significant difference between groups in the visually-guided task, but *cPcdh* $\alpha 1-12$ mice showed significantly lower performance in the memory-guided task ($**p < 0.01$). (d) Time taken to reach the correct goal. Both groups reached the goals within a few seconds in both tasks, with no significant difference. Data are presented as mean \pm SEM. Statistical significance was determined using mixed two-way ANOVA, with genotype as a between-groups factor and task as a within-groups factor.

Long-term memory retention in *cPcdh α1-12* mice assessed through fear conditioning

While short-term memory deficits have been observed in *cPcdh α1-12* mice, their impact on long-term memory remains unexplored. Given that short-term and long-term memory rely on different neural circuits and molecular mechanisms, it is important to determine whether the observed short-term impairments extend to long-term memory. To investigate this, I used a fear conditioning test to assess long-term memory. On the day of the test, each mouse freely explored the chamber for 4 min before receiving three 2 second, 0.5 mA electric shocks at 1 min intervals. Each mouse was reintroduced to the same chamber 24 h or 2 weeks later for 5 min without shocks and freezing behaviour was measured as an index of fear memory (Fig. 3a). (Fig. 3a). Both *cPcdh α1-12* and wild-type mice displayed high levels of freezing at both 24 h and 2 weeks after conditioning, indicating intact long-term memory formation at both time points (Fig. 3b).

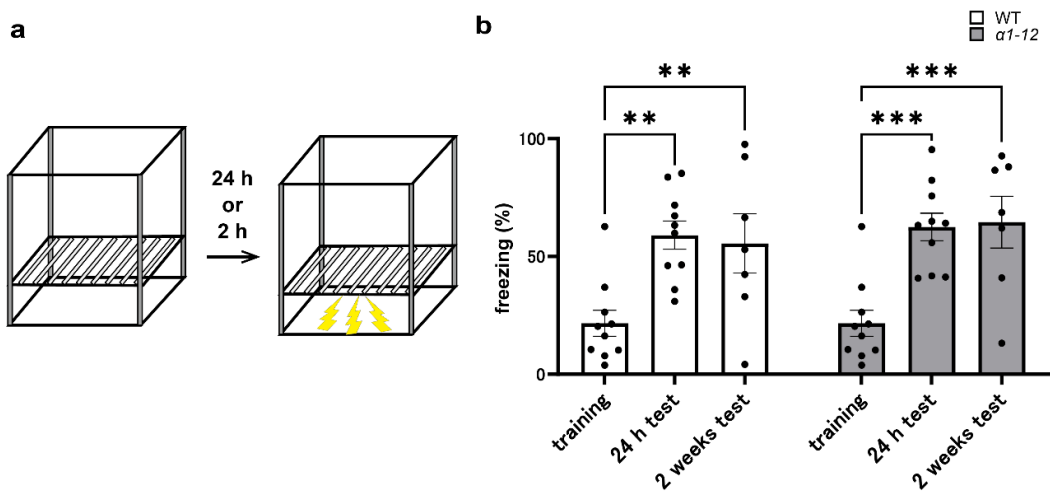


Figure 3 Fear conditioning test in *cPcdh α1-12* and wild-type mice

(a) Schematic representation of the contextual fear conditioning test. (b) Freezing response in the fear conditioning test. Both wild-type (n=10, male 5, female 5) and *cPcdh α1-12* (n=10, male 5, female 5) mice showed significant freezing at 24 h and 2 weeks, with no significant differences between genotypes. Three mice (male 2, female 1) were tested only at the 24 h time point. Data are mean \pm SEM. Statistical analysis used an independent t-test for the open field test and mixed two-way ANOVA with genotype as a between-groups factor and interval as a within-groups factor for the fear conditioning test.

Assessment of short-term and long-term associative memory in *cPcdh α1-12* mice

The standard Context Pre-exposure Facilitation Effect (CPFE) paradigm typically uses a fixed 24 h interval in which the interval between context exploration (Pre-exposure) and electric shock (Immediate Shock, IS)³⁵. In order to investigate memory formation across the different phases between short-term and long-term, I designed a modified CPFE test in which the interval between Pre-exposure and IS was fixed 2 and 24 h. Twenty-four hours after IS, the memory recall tests were administered once in the shocked context (context A) and once in another context (context B) (test 1, test 2). Freezing rates during Pre-exposure, test 1, and test 2 were quantified to assess the ability to discriminate between the two contexts (Fig. 3a). Wild-type mice exhibited significantly higher freezing rates in Test 1 compared to Test 2, regardless of the interval between Pre-exposure and IS (Fig. 3b,c). Similarly, *cPcdh α1-12* mice showed significantly increased freezing in Test 1 compared to Test 2 at the 24 h interval. However, at the 2 h interval, *cPcdh α1-12* mice showed no significant difference between Test 1 and Test 2, suggesting impaired short-term associative memory (Fig. 3b) . To confirm that this deficit was not due to differences in immediate shock responses, I measured locomotor activity immediately after IS. Both wild-type and *cPcdh α1-12* mice showed comparable levels of activity following IS, indicating that the impairment in short-term associative memory is not attributable to differences in shock-induced locomotor responses (Fig. 4d). These results indicate that although *cPcdh α1-12* mice retain

normal long-term associative memory, they exhibit specific impairments in short-term memory, which were validated within a single experimental paradigm.

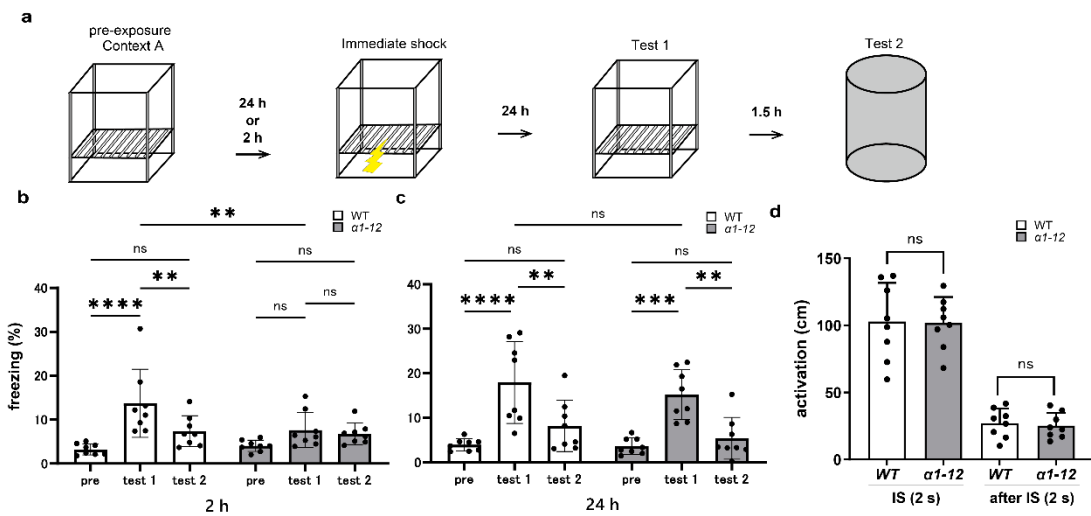


Figure 4 Short-term and long-term associative memory in *cPcdh α1-12* mice based on the CPFE test

(a) Schematic of the CPFE test protocol. The interval between Pre-exposure and Immediate Shock (IS) was set at 24 or 2 h. Memory recall Test1 was conducted 24 h after IS, followed by Test2 in a different context 1.5 h later. (b-c) Freezing response results in the CPFE test (wild-type: n=8, male 4, female 4; *cPcdh α1-12*: n=8, male 4, female 4). (b) shows the test results at the 2 h interval, and (c) shows the results at the 24 h interval. At the 24 h interval, both wild-type and *cPcdh α1-12* mice exhibited significantly higher freezing in Test 1 than in Test 2. However, at the 2 h interval, *cPcdh α1-12* mice showed no significant difference in freezing between Test 1 and Test 2. Data are presented as mean \pm SEM. Statistical significance was determined using a mixed 2-way ANOVA, with interval (2 h vs. 24 h) as a between-groups factor and phase (Pre-exposure, Test 1, Test 2) as a within-groups factor.

c-Fos analysis of neuronal activity during memory recall in *cPcdh α1-12* mice

Previous behavioral experiments have shown that *cPcdh α1-12* mice exhibit specific deficits in short-term memory, while their long-term memory retention remains intact. These results suggest that different neural circuits and molecular mechanisms may be involved in short-term and long-term memory. To further investigate, I next analyzed neuronal activity during memory recall using c-Fos staining, a marker for neuronal activation, to examine which brain regions are associated with these memory impairments at the cellular level. Mice were sacrificed 1.5 h after being placed in context A, and brain tissues were processed for c-Fos staining. For detailed analysis of neuronal activity, coronal sections were prepared along the anterior-posterior axis of the brain, and quantitative analyses were performed on each section. c-Fos-positive cells were automatically detected, and the obtained brain sections were registered with the Allen Brain Atlas using Serial Section Registration^{47,48}. For each mouse, 96 coronal sections from AP 2.3 to AP -4.0 were analyzed to assess neuronal activity across the anterior-posterior axis (Fig. 5a). In tests conducted at a 2 h interval, c-Fos-positive neurons were observed in wild-type mice across multiple cortical and subcortical regions, including the hippocampus, prefrontal cortex, and basolateral amygdala, indicating that these areas are strongly involved in memory recall. These results were consistent with the active regions observed in conventional CPFE tests conducted previously^{49,50}. In contrast, *cPcdh α1-12* mice showed significantly reduced neuronal activity

during recall in regions such as the hippocampus (CA1, CA3), retrosplenial area (RSP), amygdala (MEA, BLA), and endopiriform nucleus (EP), compared to wild-type mice (Fig. 5b, d (i-v), e, Fig 6. a). These findings are consistent with the behavioral experiments and suggest that the specific impairments in short-term memory recall observed in *cPcdh α1-12* mice may be caused at the neuronal level. Furthermore, when tested at a 24 h interval, no significant differences in c-Fos-positive neuronal activity were observed between *cPcdh α1-12* mice and wild-type mice in the hippocampus, prefrontal cortex, amygdala, and other mentioned brain regions (Fig. 5c, c (i'-v'), e, Fig. 6 b). These findings indicate that while *cPcdh α1-12* mice exhibit abnormal neuronal activity related to short-term memory, their neuronal activity during long-term memory recall appears to be normal.

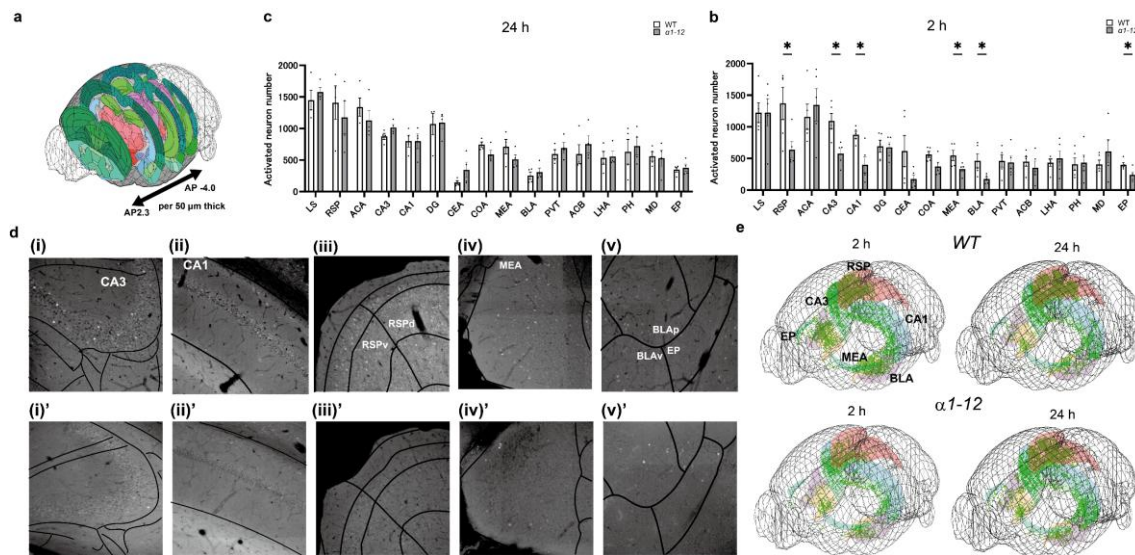


Figure 5 Comparison of neuronal activity in brain regions during short-term and long-term memory recall in *cPcdh α1-12* mice

(a) Coronal brain sections (50 μ m thick, AP 2.3 to AP -4.0) were prepared and aligned with the Allen Brain Atlas for c-Fos quantification. 2 h interval *cPcdh α1-12* (n=5, male 3, female 2), wild-type (n=5, male 3, female 2), 24 h interval *cPcdh α1-12* (n=4, male 2, female 2), wild-type (n=4, male 2, female 2). Approximately 98 slices were obtained per mouse. (b) Quantification of c-Fos-positive neurons in brain regions of *cPcdh α1-12* mice and wild-type mice tested at a 24 h interval. The top 16 regions with the highest number of cells in wild-type mice are shown. No significant differences were observed between wild-type and *cPcdh α1-12* mice across any of the brain regions. (c) Quantification of c-Fos-positive neurons in brain regions of *cPcdh α1-12* and wild-type mice tested at a 2 h interval. In *cPcdh α1-12* mice, significantly fewer c-Fos-positive neurons were observed in the hippocampus (CA1, CA3), retrosplenial area (RSPd, RSPv), amygdala (MEA, BLA), and endopiriform nucleus (EP) compared to wild-type mice. Statistical significance is indicated by *p < 0.05. (d) Representative images of c-Fos staining observed in *cPcdh α1-12* (i'-vi') and wild-type mice (i-vi) 2 h after memory recall. (i), (i') CA3 (ii), (ii') CA1 (iii), (iii') RSP (iv), (iv') MEA (v), (v') BLA, EP. Scale bar = 100 μ m. (e) 3D reconstruction of c-Fos-positive neurons. Activated neurons (green dots) are visualized in regions where *cPcdh α1-12* mice showed significantly reduced activity, highlighting the differences in neuronal activity patterns between the 4 groups. Data are presented as mean \pm SEM. Statistical significance was determined using unpaired t-test.

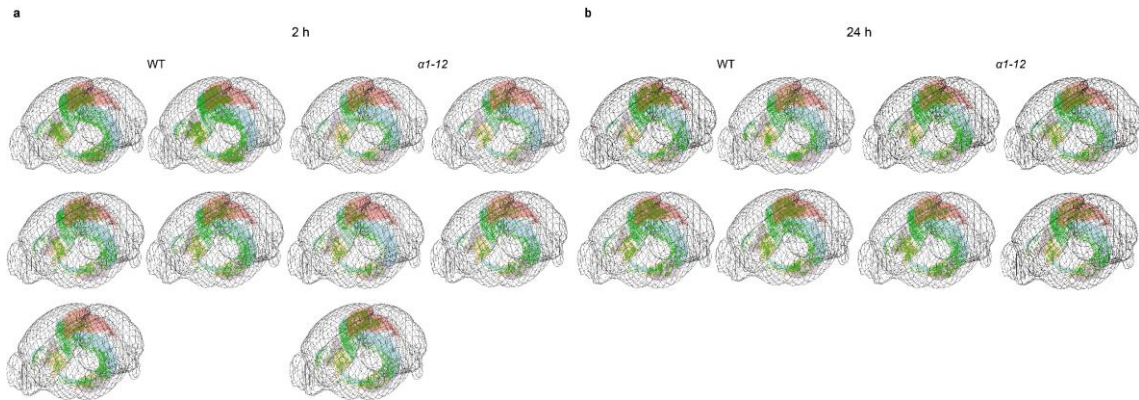


Figure 6 Spatial distribution of c-Fos-positive neurons in wild-type and *cPcdh-α1-12* mice at 2 h and 24 h intervals

(a) 3D reconstructions of c-Fos-positive neuronal distributions in wild-type and *cPcdh-α1-12* mice 2 h after memory recall. Each dot represents the location of a c-Fos-positive neuron, visualizing the distribution of activated neurons.(b) 3D reconstructions of c-Fos-positive neuronal distributions in wild-type and *cPcdh-α1-12* mice 24 h after memory recall. Color coding represents different brain regions: red for the RSP, green for CA3, and blue for the CA1, yellow for the MEA, and purple for the BLA. The wireframe outlines denote the brain structure for anatomical reference.

Differential neural circuits involved in short-term and long-term memory recall

In this study, *cPcdh α1-12* mice showed a significant reduction in neural activity during short-term memory recall at the 2 h interval, whereas neural activity at the 24 h interval remained comparable between groups. These findings indicate that distinct neural circuits may be engaged during memory recall at different time intervals. To further investigate this, I compared overall neuronal activation across subjects and conducted a regional analysis of neuronal activity. For each brain region, I quantified c-Fos expression across a 500 μm anterior-posterior range. At the 2 h interval, *cPcdh α1-12* mice exhibited significantly reduced neuronal activity, confirming significant reductions in these regions. Neuronal activity in CA3, BLA, and RSP was significantly elevated during short-term memory recall compared to long-term recall (Fig. 7a-c), whereas neuronal activity remained unchanged in CA1, MEA, and EP (Fig. 7d-f). In contrast, *cPcdh α1-12* mice exhibited a reversed pattern, with significantly lower neuronal activity across all six regions at the 2 h interval relative to the 24 h interval. These results indicate that CA3, BLA, and RSP are crucial for short-term memory recall and that their reduced neuronal activity in *cPcdh α1-12* mice reflects dysfunction in short-term memory-related neural circuits.

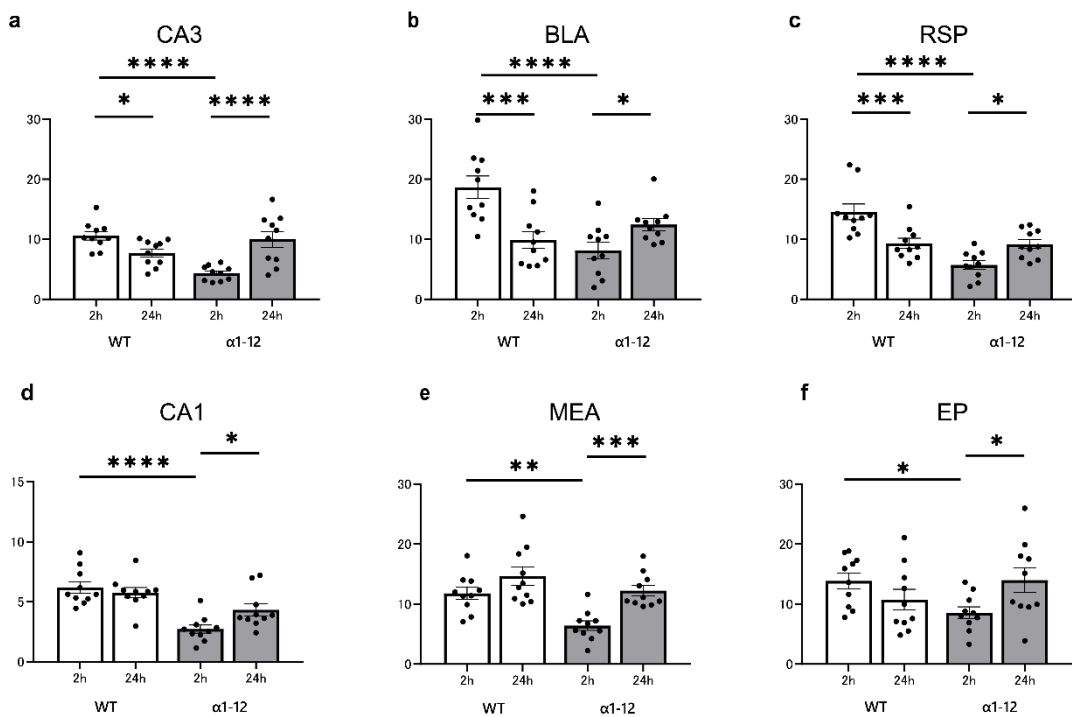


Figure 7 Slice comparison of neural activity at 2 h and 24 h in wild-type and *cPcdh α1-12* mice

c-Fos expression in six brain regions in wild-type and *cPcdh α1-12* mice. (a) CA3, (b) BLA, (c) RSP, (d) CA1, (e) MEA, and (f) EP. Each point on the bar graph represents the mean value of c-Fos-positive neurons from corresponding sections on the same Atlas. 2 h interval: *cPcdh α1-12* (n = 5, male 3, female 2), wild-type (n = 5, male 3, female 2). 24 h interval: *cPcdh α1-12* (n = 4, male 2, female 2), wild-type (n = 4, male 2, female 2). For each region, 10 coronal sections (50 μ m thick) were analyzed. Data are presented as mean \pm SEM. Statistical significance was determined using a mixed 2-way ANOVA, with genotype as a between-groups factor and interval (2 h vs. 24 h) as a within-groups factor.

Discussion

***cPcdh α1-12* mice exhibit short-term memory deficits but retain normal long-term memory.**

In this study, I conducted a detailed analysis of how the diversity of *cPcdh α* affects short-term and long-term memory. The results indicated that while *cPcdh α1-12* mice exhibited deficits in short-term memory, long-term memory was not significantly affected. Specifically, in the T-maze task and CPFE test, *cPcdh α1-12* mice performed significantly worse than wild-type mice in tasks requiring short-term memory, demonstrating difficulties in retaining information for short periods and distinguishing contexts. While there is some concern that genetic background differences may have influenced these phenotypes, *cPcdh α1-12* mice were generated on a C57BL/6 background³⁴ and maintained as a separate colony from control C57BL/6J mice in the same room under identical environmental conditions. These findings suggest that the molecular diversity of *cPcdh α* plays a crucial role in the formation and function of neural circuits.

2 h interval is commonly employed in the study of short-term memory in rodents^{21,22}. However, interpreting the results requires careful consideration. Firstly, while the 2 h interval is generally considered to involve short-term memory, some studies suggest that it may also encompass processes distinct from those involved in very short-term memory, which lasts less than one hour, or long-term memory, which lasts more than one day. Therefore, the reduced

freezing observed in *cPcdh α1-12* mice in the two-hour condition may indicate an issue with the formation of short-term or intermediate memory. Secondly, this study did not control the time of day. Many reports have shown that memory performance and hippocampal function can change depending on the internal circadian phase⁵¹. The state of the internal clock at the time of context exposure, shock or testing may have influenced memory processing in the two conditions. Thirdly, in our CPFE design, we varied the time between exposure to the context and the shock in order to test for differences in memory formation. However, behavioral tests were conducted twenty-four hours after the shock for both groups. Consequently, the freezing responses reflect memories retained for a full day in both cases. The lower freezing response observed in the two-hour group does not simply indicate a failure of short-term memory. Instead, it may indicate an inability to establish a strong association that could be recalled the following day. Although the two-hour interval likely involved short-term memory processes at the time of the shock, the behavior we measured depended on long-term retention. Our findings suggest that short-term associative memory formation is impaired in *cPcdh α1-12* mice, but further studies are needed to distinguish clearly between early memory formation and later memory retention. Finally, sleep may have influenced the results. The twenty-four-hour condition probably included multiple sleep periods, whereas the two-hour condition allowed less time for sleep. However, short sleep episodes may still have occurred in both groups. Nevertheless, short sleep episodes may still have occurred in

both groups. Since sleep is known to stabilize and reorganize memories, differences in sleep exposure may have contributed to the differences in memory performance between the two conditions.

Short-term memory deficits and neural activity patterns

Short-term memory deficits were further corroborated by analyses of neuronal activity using c-Fos staining. In conditions requiring short-term memory, *cPcdh α1-12* mice showed significantly reduced neuronal activity in brain regions such as the hippocampus, amygdala, and retrosplenial cortex. In contrast, in tests conducted 24 h later, no significant differences in neuronal activity were observed between *cPcdh α1-12* mice and wild-type mice, indicating that normal neural activity was maintained in long-term memory. This reduction in neuronal activity during short-term memory tasks aligns with the observed behavioral deficits and provides further evidence of direct impairments in cellular activity in *cPcdh α1-12* mice. The hippocampus, amygdala, and retrosplenial cortex each play distinct but interconnected roles in memory processing: the hippocampus is involved in encoding and retrieving episodic memory¹⁻⁶, the amygdala contributes to emotional and associative memory^{7,9,13}, and the retrosplenial cortex integrates spatial and contextual information¹⁵. These regions are interconnected through neural circuits, functioning in a coordinated manner to support memory retention^{2,20,52}. These findings strongly support the idea that the reduced neuronal activity observed in *cPcdh α1-12* mice reflects

not just localized dysfunction but a disruption in circuit-wide coordination. The short-term memory deficits are likely driven by direct impairments in cellular function.

Molecular mechanisms underlying short-term memory deficits in *cPcdh α1-12* mice

The observation that *cPcdh α1-12* mice exhibit impairments in short-term memory while retaining normal long-term memory suggests that short-term and long-term memories are not merely sequential stages of a unified process but instead rely on partially independent molecular pathways. This distinction between short-term and long-term memories is further supported by findings from multiple levels of analysis, as knockout mice lacking PKC-gamma, which regulates critical aspects of synaptic plasticity and memory, or brevican, a major component of perineuronal nets that stabilizes synaptic connections and modulates neural plasticity, also exhibit selective impairments in short-term memory^{22,53}. Additionally, pharmacological studies have demonstrated that inhibition of specific hippocampal receptors selectively disrupts short-term memory while sparing long-term memory²¹, reinforcing the notion that distinct molecular mechanisms govern these processes. Together, these findings consistently support the functional separation of short-term and long-term memories across engram, synaptic, and pharmacological levels. In this study, neuronal activity in the hippocampal CA3, BLA, and RSP of wild-type mice significantly increased during memory recall at a 2 h-interval, suggesting that these regions play a key role in short-term memory retention. These results also support the

idea that, while short-term and long-term memory share neural circuits, they depend on distinct molecular mechanisms.

Clustered protocadherins, including those in the *cPcdh α* family, have been identified as cell adhesion molecules localized at synaptic junctions, where they contribute to synapse formation and stabilization²⁵. Synaptic modifications that support short-term memory heavily depend on the regulation of cell adhesion molecules, which mediate synapse formation and structural remodeling in response to neuronal activity. Notably, adhesion molecules such as NCAM and FasII have been shown to be associated with synaptic plasticity and transient synaptic modifications and are specifically involved in processes related to short-term memory.^{21,54-57}. A potential explanation for the short-term memory deficits in *cPcdh α1-12* mice is that *cPcdhs*, as cell adhesion molecules, play a key role in regulating synaptic remodeling. On the other hand, the molecular diversity of *cPcdhs* has been shown to contribute to self-avoidance during dendritic synapse formation^{58,59} and is also considered essential for the formation of specific neural circuits between different neurons^{60,61}. These findings suggest that the reduced molecular diversity of *cPcdh α* disrupts the specificity of *cPcdh*-dependent synaptic formation, potentially impairing the formation of specialized neural circuits required for short-term memory in *cPcdh α1-12* mice.

Role of *cPcdh α* diversity in neural circuit formation

Previous research has shown that the molecular diversity of *cPcdh* contributes to the formation of neural circuits and the specificity of intercellular adhesion. This study newly demonstrates that this diversity is critical for the function of neural circuits, particularly in short-term memory formation. Because *cPcdh α1-12* mice lack *cPcdh α* diversity, specific interactions within neural circuit connectivity may be limited, resulting in short-term memory impairments. This finding suggests that specific neural circuits are vital for short-term information retention and that the diversity of *cPcdh α* is essential for their formation.

Additionally, given that *cPcdhs* contribute to neural circuit formation, their dysfunction has been implicated in neurodevelopmental and neuropsychiatric disorders⁶²⁻⁶⁶. Mutations in *cPcdh* genes have been linked to autism spectrum disorder⁶⁷ and schizophrenia⁶⁸⁻⁷⁰, both of which involve cognitive and memory deficits. The findings of this study suggest that the loss of *cPcdh α* diversity impairs synaptic plasticity and memory retention, potentially providing insights into how protocadherin dysfunction contributes to cognitive impairments in these disorders. Investigating the role of *cPcdh α* diversity in synaptic plasticity across different brain regions may further elucidate its contributions to neurodevelopmental conditions.

Material and methods

Animal experiments

All the experimental procedures were in accordance with the Guide for the Care and Use of Laboratory Animals of the Science Council of Japan and were approved by the Animal Experiment Committee of Osaka University. After the experiments, mice were anaesthetized with isoflurane to ensure minimal distress. Euthanasia was performed by cervical dislocation, in compliance with institutional animal care and use guidelines. All procedures adhered to the ARRIVE guidelines.

Animal Model Preparation

All experiments used C57BL/6 mice and *cPcdh α1-12* mice (BRC No. RBRC02798), which were generated and characterized according to the method described previous research⁷¹. They were from our own breeding stock and housed in groups of 5 – 8 mice per cage. The mice used in the experiments were 2 to 4 months old, including both male and female animals. The animals were housed at a temperature of $23 \pm 1^\circ\text{C}$ with $50\% \pm 10\%$ relative humidity under a 12 h light/dark cycle (lights on at 8:00 a.m., lights off at 8:00 p.m.). Prior to the experiments, all mice were handled for 5 min per day and transitioned to individual housing starting three days before the experiments to acclimate them to the experimental environment. Prior to the experiments, all

mice were handled for 5 min per day to minimize handling stress. Mice were transitioned to individual housing starting three days before the experiments for the following reasons. This approach aimed to minimize the influence of social interactions with other mice on c-Fos expression and to reduce variability among individuals caused by such interactions.

Behavioral Experiments

The activity levels of individually housed mice in their home cages were measured using an implantable nanotag (Kissei Comtec Co., Tokyo, Japan). This device includes a triaxial accelerometer that continuously detects animal movement without restraining the subject. In this study, the manufacturer's recommended threshold settings were used with a recording interval of 5 min. Each mouse was monitored for 14 days, and the activity levels of wild-type mice ($n = 2$) and *cPcdh α1-12* mice ($n = 2$) were compared.

The open field test was conducted to evaluate spontaneous locomotor activity and anxiety-like behavior in mice. Testing was carried out in a white acrylic open field box (50 cm \times 50 cm \times 40 cm) cleaned with 70% ethanol between trials to minimize odor cues. Each mouse was placed in the center of the box and allowed to explore freely for 60 min. Mouse behavior was recorded by an overhead video camera at 30 frames per second, and the time spent in the central area and total distance traveled was used as assessment metrics. An increase in time spent in the

center was used as an indicator of reduced anxiety, while the total distance traveled was used as an indicator of spontaneous locomotor activity. Mouse movements were analyzed using DeepLabCut, a deep-learning-based markerless tracking tool ⁷². The nose tip, right ear, left ear, and tail base were tracked to calculate movement trajectories. The central area was defined as the inner 25 cm × 25 cm square, and the time spent in this area was calculated as a percentage of the total exploration time. The total distance traveled was computed by summing the displacement of the tracked points frame by frame. All analyses were conducted using MATLAB software.

The contextual fear conditioning test was conducted to evaluate fear memory in mice. Testing was carried out in a conditioning chamber measuring 30 cm × 24 cm × 21 cm, equipped with a stainless-steel grid floor for administering electric shocks. The chamber was cleaned with 70% ethanol between trials to minimize odor cues. Additionally, the chamber was placed inside a soundproof box (51 × 51 × 34 cm) with dim lighting. In this between-subjects design, each mouse was placed in the chamber on the test day and allowed to explore freely for 4 min, followed by three 2 sec electric shocks of 0.5 mA, administered at 1 min intervals. After 24 h or 2 weeks, each mouse was reintroduced to the same chamber for 5 min without electric shocks, and the percentage of freezing responses was recorded as an index of fear memory. Freezing was defined as the state in which each of the four tracked points remained within a 0.8 cm radius for a minimum of 2 sec. The freezing percentage was calculated using MATLAB. Automated

measurements were validated by comparison with manual visual scoring, confirming no significant differences between the two methods.

CPFE test was conducted to assess the formation of contextual memory. Testing was conducted in a conditioning chamber measuring 30 cm × 24 cm × 21 cm, with two distinct contexts, context A and context B. In context A, a square tube (19.8 × 19.8 × 21 cm) covered with paper was used, while in context B, an acrylic cylindrical tube (22 cm diameter, 21 cm height) was set up. The chamber was cleaned with 70% ethanol between trials to minimize odor cues. On the day before the test, each mouse was pre-exposed to context A for 5 min. Two or twenty-four h after pre-exposure, each mouse was reintroduced to the chamber, and a 0.5 mA electric shock (2 sec) was administered 5 sec after placement. After 1 min, each mouse was removed from the chamber. Twenty-four h after conditioning, each mouse was placed in context A for 5 min and allowed to move freely, followed by a 5 min placement in context B 1.5 h later. Freezing responses were recorded as an index of contextual memory.

T-maze test was conducted to assess short-term memory of visuospatial information. The T-maze was constructed from black plastic with arms measuring 30 cm wide, 100 cm long, 10 cm high, and with a passage width of 5 cm. White plastic cues (5 cm width × 10 cm height) were placed either at the choice point or 10 cm from the starting point. Training and testing began when mice were 2 months old. Each correct trial was rewarded with 50 µl of a 5% glucose solution,

while in incorrect trials, the mice were reintroduced to the correct arm. Trials were terminated if a mouse failed to choose an arm within 4 min of placement in the maze. Each mouse performed 20 trials per day and consumed 1 mL of the 5% glucose solution per session. To maintain motivation for the reward, mice were housed under intermittent water restriction. The first session began two days after the start of water deprivation, and mice were trained for a maximum of five consecutive days before water deprivation was discontinued. The training duration varied among mice to ensure that their body weight was maintained at approximately 85% of their pre-deprivation weight while allowing for normal body growth throughout the intermittent water deprivation period. Adjustments in training duration were made as needed to balance effective task learning with maintaining the health and well-being of the animals.

Tissue Preparation and acquisition of serial sections

Mice were anaesthetized with isoflurane, perfused transcardially first with 25 mm PBS and then with 4% paraformaldehyde (PFA) in PB (pH 7.3). The brains, removed from the skull, were stored in PFA at 4°C overnight, then transferred to 25 mm PBS with 30% sucrose and kept at 4°C overnight. Brains were embedded in a cryomold (Tissue-Tek) with the cortex facing upwards, using a mixture of OCT compound (Tissue-Tek) and 30% sucrose at a 2:1 ratio. The samples were frozen in isopentane cooled with liquid nitrogen and sectioned coronally at 50 μ m thickness using a cryostat (CM3050S, Leica).

Immunohistochemistry

Sections were washed with 25 mM PBS, and a blocking solution (500 μ l per well) was applied for 1 h at room temperature to prevent non-specific binding. Sections were then incubated overnight at 4°C with a 1:1000 dilution of the primary antibody (rabbit anti-c-Fos, *Cell Signaling Technology*) in blocking solution. After washing with 25 mM PBS, sections were incubated with a 1:1000 dilution of the secondary antibody (AlexaFluor488, *Invitrogen*) in PBS with 0.1% Triton X-100 for 2 h at room temperature. Following the secondary antibody incubation, the plate was shielded from light with aluminum foil. Sections were then washed in 25 mM PBS, mounted on glass slides (MAS-01, MATSUNAMI), covered with antifade mounting medium (Immunoselect Antifading Mounting Medium, dianovaTM), and sealed with nail polish.

Cell Counting

The localization and number of cells were quantified semi-automatically using MATLAB. c-Fos-positive cells were defined as bright spots with a radius of 3-4 pixels and a brightness above a threshold that matched visual counting in randomly selected images with an agreement of 95% or more. Images were deformed to align 40-60 landmark points on each section to account for shifts due to section distortion or damage, thereby ensuring precise cell localization based on the Allen Mouse Brain Common Coordinate Framework (CCFv3)^{47,48}.

Data Analysis

GraphPad Prism was used for data analysis. All graphs present data as mean \pm SEM, and statistical significance was set at * $p < 0.05$, ** $p < 0.01$, *** $p < 0.001$, *** $p < 0.0001$.

References

1. Ramirez, S. *et al.* Activating positive memory engrams suppresses depression-like behaviour. *Nature* **522**, 335–339 (2015).
2. Ryan, T. J., Roy, D. S., Pignatelli, M., Arons, A. & Tonegawa, S. Memory. Engram cells retain memory under retrograde amnesia. *Science* **348**, 1007–1013 (2015).
3. Ohkawa, N. *et al.* Artificial association of pre-stored information to generate a qualitatively new memory. *Cell Rep* **11**, 261–269 (2015).
4. Redondo, R. L. *et al.* Bidirectional switch of the valence associated with a hippocampal contextual memory engram. *Nature* **513**, 426–430 (2014).
5. Ramirez, S. *et al.* Creating a false memory in the hippocampus. *Science* **341**, 387–391 (2013).
6. Liu, X. *et al.* Optogenetic stimulation of a hippocampal engram activates fear memory recall. *Nature* **484**, 381–385 (2012).
7. Gore, F. *et al.* Neural Representations of Unconditioned Stimuli in Basolateral Amygdala Mediate Innate and Learned Responses. *Cell* **162**, 134–145 (2015).
8. Zelikowsky, M., Hersman, S., Chawla, M. K., Barnes, C. A. & Fanselow, M. S. Neuronal ensembles in amygdala, hippocampus, and prefrontal cortex track differential components of contextual fear. *J Neurosci* **34**, 8462–8466 (2014).

9. Reijmers, L. G., Perkins, B. L., Matsuo, N. & Mayford, M. Localization of a stable neural correlate of associative memory. *Science* **317**, 1230–1233 (2007).
10. Hsiang, H.-L. L. *et al.* Manipulating a ‘cocaine engram’ in mice. *J Neurosci* **34**, 14115–14127 (2014).
11. Yiu, A. P. *et al.* Neurons are recruited to a memory trace based on relative neuronal excitability immediately before training. *Neuron* **83**, 722–735 (2014).
12. Kim, J., Kwon, J.-T., Kim, H.-S., Josselyn, S. A. & Han, J.-H. Memory recall and modifications by activating neurons with elevated CREB. *Nat Neurosci* **17**, 65–72 (2014).
13. Zhou, Y. *et al.* CREB regulates excitability and the allocation of memory to subsets of neurons in the amygdala. *Nat Neurosci* **12**, 1438–1443 (2009).
14. Han, J.-H. *et al.* Selective erasure of a fear memory. *Science* **323**, 1492–1496 (2009).
15. Cowansage, K. K. *et al.* Direct reactivation of a coherent neocortical memory of context. *Neuron* **84**, 432–441 (2014).
16. Kitamura, T. *et al.* Engrams and circuits crucial for systems consolidation of a memory. *Science* **356**, 73–78 (2017).
17. Goto, A. *et al.* Stepwise synaptic plasticity events drive the early phase of memory consolidation. *Science* **374**, 857–863 (2021).

18. Saneyoshi, T. *et al.* Reciprocal Activation within a Kinase-Effector Complex Underlying Persistence of Structural LTP. *Neuron* **102**, 1199-1210.e6 (2019).
19. Preston, A. R. & Eichenbaum, H. Interplay of Hippocampus and Prefrontal Cortex in Memory. *Current Biology* **23**, R764–R773 (2013).
20. Tonegawa, S., Morrissey, M. D. & Kitamura, T. The role of engram cells in the systems consolidation of memory. *Nat Rev Neurosci* **19**, 485–498 (2018).
21. Izquierdo, I. *et al.* Mechanisms for memory types differ. *Nature* **393**, 635–636 (1998).
22. Gomis-González, M. *et al.* Protein Kinase C-Gamma Knockout Mice Show Impaired Hippocampal Short-Term Memory While Preserved Long-Term Memory. *Mol Neurobiol* **58**, 617–630 (2021).
23. Hernandez, P. J. & Abel, T. The role of protein synthesis in memory consolidation: progress amid decades of debate. *Neurobiol Learn Mem* **89**, 293–311 (2008).
24. Dudai, Y., Karni, A. & Born, J. The Consolidation and Transformation of Memory. *Neuron* **88**, 20–32 (2015).
25. Kohmura, N. *et al.* Diversity Revealed by a Novel Family of Cadherins Expressed in Neurons at a Synaptic Complex. *Neuron* **20**, 1137–1151 (1998).

26. Wu, Q. & Maniatis, T. A Striking Organization of a Large Family of Human Neural Cadherin-like Cell Adhesion Genes. *Cell* **97**, 779–790 (1999).
27. Yagi, T. & Takeichi, M. Cadherin superfamily genes: functions, genomic organization, and neurologic diversity. *Genes Dev.* **14**, 1169–1180 (2000).
28. Wu, Q. *et al.* Comparative DNA Sequence Analysis of Mouse and Human Protocadherin Gene Clusters. *Genome Res.* **11**, 389–404 (2001).
29. Tasic, B. *et al.* Promoter Choice Determines Splice Site Selection in Protocadherin α and γ Pre-mRNA Splicing. *Molecular Cell* **10**, 21–33 (2002).
30. Wang, X., Su, H. & Bradley, A. Molecular mechanisms governing Pcdh-gamma gene expression: evidence for a multiple promoter and cis-alternative splicing model. *Genes Dev.* **16**, 1890–1905 (2002).
31. Kaneko, R. *et al.* Allelic gene regulation of Pcdh-alpha and Pcdh-gamma clusters involving both monoallelic and biallelic expression in single Purkinje cells. *J Biol Chem* **281**, 30551–30560 (2006).
32. Schreiner, D. & Weiner, J. A. Combinatorial homophilic interaction between gamma-protocadherin multimers greatly expands the molecular diversity of cell adhesion. *Proc Natl Acad Sci U S A* **107**, 14893–14898 (2010).

33. Thu, C. A. *et al.* Single-cell identity generated by combinatorial homophilic interactions between α , β , and γ protocadherins. *Cell* **158**, 1045–1059 (2014).

34. Noguchi, Y. *et al.* Total expression and dual gene-regulatory mechanisms maintained in deletions and duplications of the Pcdha cluster. *J Biol Chem* **284**, 32002–32014 (2009).

35. Rudy, J. W., Huff, N. C. & Matus-Amat, P. Understanding contextual fear conditioning: insights from a two-process model. *Neuroscience & Biobehavioral Reviews* **28**, 675–685 (2004).

36. Bassett, D. S. & Sporns, O. Network neuroscience. *Nat Neurosci* **20**, 353–364 (2017).

37. Sano, K. *et al.* Protocadherins: a large family of cadherin-related molecules in central nervous system. *EMBO J* **12**, 2249–2256 (1993).

38. Brasch, J. *et al.* Visualization of clustered protocadherin neuronal self-recognition complexes. *Nature* **569**, 280 (2019).

39. Goodman, K. M. *et al.* Protocadherin cis-dimer architecture and recognition unit diversity. *Proceedings of the National Academy of Sciences* **114**, E9829–E9837 (2017).

40. Goodman, K. M. *et al.* γ -Protocadherin structural diversity and functional implications. *eLife* **5**, e20930 (2016).
41. Goodman, K. M. *et al.* Structural Basis of Diverse Homophilic Recognition by Clustered α - and β -Protocadherins. *Neuron* **90**, 709–723 (2016).
42. Fukuda, E. *et al.* Down-regulation of protocadherin-alpha A isoforms in mice changes contextual fear conditioning and spatial working memory. *Eur J Neurosci* **28**, 1362–1376 (2008).
43. Asai, H. *et al.* Pcdh β deficiency affects hippocampal CA1 ensemble activity and contextual fear discrimination. *Molecular Brain* **13**, 7 (2020).
44. Esumi, S. *et al.* Monoallelic yet combinatorial expression of variable exons of the protocadherin-alpha gene cluster in single neurons. *Nat Genet* **37**, 171–176 (2005).
45. Yoshitake, K. *et al.* Visual Map Shifts based on Whisker-Guided Cues in the Young Mouse Visual Cortex. *Cell Reports* **5**, 1365–1374 (2013).
46. Yamagishi, T. *et al.* Molecular diversity of clustered protocadherin- α required for sensory integration and short-term memory in mice. *Sci Rep* **8**, 9616 (2018).
47. Chen, S. *et al.* High-Throughput Strategy for Profiling Sequential Section With Multiplex Staining of Mouse Brain. *Front Neuroanat* **15**, 771229 (2021).

48. Wang, Q. *et al.* The Allen Mouse Brain Common Coordinate Framework: A 3D Reference Atlas. *Cell* **181**, 936-953.e20 (2020).

49. Rudy, J. W. Context representations, context functions, and the parahippocampal-hippocampal system. *Learn. Mem.* **16**, 573–585 (2009).

50. Schiffino, F. L., Murawski, N. J., Rosen, J. B. & Stanton, M. E. Ontogeny and neural substrates of the context preexposure facilitation effect. *Neurobiol Learn Mem* **95**, 190–198 (2011).

51. Eckel-Mahan, K. L. *et al.* Circadian oscillation of hippocampal MAPK activity and cAMP: implications for memory persistence. *Nat Neurosci* **11**, 1074–1082 (2008).

52. Sun, W. *et al.* Spatial transcriptomics reveal neuron–astrocyte synergy in long-term memory. *Nature* **627**, 374–381 (2024).

53. Favuzzi, E. *et al.* Activity-Dependent Gating of Parvalbumin Interneuron Function by the Perineuronal Net Protein Brevican. *Neuron* **95**, 639-655.e10 (2017).

54. Martin, K. C. & Kandel, E. R. Cell Adhesion Molecules, CREB, and the Formation of New Synaptic Connections. *Neuron* **17**, 567–570 (1996).

55. Sutton, M. A., Masters, S. E., Bagnall, M. W. & Carew, T. J. Molecular mechanisms underlying a unique intermediate phase of memory in aplysia. *Neuron* **31**, 143–154 (2001).

56. Trannoy, S., Redt-Clouet, C., Dura, J.-M. & Preat, T. Parallel Processing of Appetitive Short- and Long-Term Memories In *Drosophila*. *Current Biology* **21**, 1647–1653 (2011).
57. Izquierdo, L. A. *et al.* Molecular pharmacological dissection of short- and long-term memory. *Cell Mol Neurobiol* **22**, 269–287 (2002).
58. Rubinstein, R. *et al.* Molecular logic of neuronal self-recognition through protocadherin domain interactions. *Cell* **163**, 629–642 (2015).
59. Lefebvre, J. L., Kostadinov, D., Chen, W. V., Maniatis, T. & Sanes, J. R. Protocadherins mediate dendritic self-avoidance in the mammalian nervous system. *Nature* **488**, 517–521 (2012).
60. Yagi, T. Genetic basis of neuronal individuality in the mammalian brain. *J Neurogenet* **27**, 97–105 (2013).
61. Tarusawa, E. *et al.* Establishment of high reciprocal connectivity between clonal cortical neurons is regulated by the Dnmt3b DNA methyltransferase and clustered protocadherins. *BMC Biol* **14**, 103 (2016).
62. Iacono, G. *et al.* Increased H3K9 methylation and impaired expression of Protocadherins are associated with the cognitive dysfunctions of the Kleefstra syndrome. *Nucleic Acids Res* **46**, 4950–4965 (2018).

63. Naskar, T. *et al.* Ancestral Variations of the PCDHG Gene Cluster Predispose to Dyslexia in a Multiplex Family. *EBioMedicine* **28**, 168–179 (2018).
64. Li, Y. *et al.* Synaptic Adhesion Molecule Pcdh- γ C5 Mediates Synaptic Dysfunction in Alzheimer's Disease. *J Neurosci* **37**, 9259–9268 (2017).
65. El Hajj, N., Dittrich, M. & Haaf, T. Epigenetic dysregulation of protocadherins in human disease. *Semin Cell Dev Biol* **69**, 172–182 (2017).
66. El Hajj, N. *et al.* Epigenetic dysregulation in the developing Down syndrome cortex. *Epigenetics* **11**, 563–578 (2016).
67. Anitha, A. *et al.* Protocadherin α (PCDHA) as a novel susceptibility gene for autism. *J Psychiatry Neurosci* **38**, 192–198 (2013).
68. Shao, Z. *et al.* Dysregulated protocadherin-pathway activity as an intrinsic defect in induced pluripotent stem cell-derived cortical interneurons from subjects with schizophrenia. *Nat Neurosci* **22**, 229–242 (2019).
69. Schizophrenia Working Group of the Psychiatric Genomics Consortium. Biological insights from 108 schizophrenia-associated genetic loci. *Nature* **511**, 421–427 (2014).
70. Pedrosa, E. *et al.* Analysis of protocadherin alpha gene enhancer polymorphism in bipolar disorder and schizophrenia. *Schizophr Res* **102**, 210–219 (2008).

71. Noguchi, Y. *et al.* Total Expression and Dual Gene-regulatory Mechanisms Maintained in Deletions and Duplications of the *Pcdha* Cluster*. *Journal of Biological Chemistry* **284**, 32002–32014 (2009).
72. Mathis, A. *et al.* DeepLabCut: markerless pose estimation of user-defined body parts with deep learning. *Nat Neurosci* **21**, 1281–1289 (2018).

Acknowledgments

I would like to express my sincere gratitude to Professor Yagi of the Kokoro Laboratory, Graduate School of Frontier Biosciences, Osaka University, for their enthusiastic support and guidance throughout the course of this study. I have had the support and encouragement of the staff of this laboratory for their appropriate technical advice. Professor Kitazawa and Professor Tachibana of the same Graduate School, and Professor Yasohima of the same university give insightful comments and suggestions.

Accomplishments

1. Peer-reviewed paper

- [1] **Tomoki Osuka**, Hiroki Yamamoto, and Takeshi Yagi. "Diversity of clustered protocadherin- α genes in neuronal identity and its role in short-term specific associative memory formation." *Scientific Reports* 15.1 (2025)
- [2] Nanami Kawamura, **Tomoki Osuka**, Ryosuke Kaneko, Eri Kishi, Ryuon Higuchi, Yumiko Yoshimura, Takahiro Hirabayashi, Takeshi Yagi and Etsuko Tarusawa : "Reciprocal Connections between Parvalbumin-Expressing Cells and Adjacent Pyramidal Cells Are Regulated by Clustered Protocadherin γ ." *eneuro* 10.10 (2023)

2. Conference presentation

- [2] Yuki Ito, **Tomoki Osuka**, Kohta I. Kobayashi, "Detection performance improves based on the three principles of audiovisual integration in head-fixed Mongolian gerbil", SfN(Society for Neuroscience) Global Connectome: A Virtual Event, 2021 年 1 月
- [3] **Tomoki Osuka** , Ryuon Higuchi , Takeshi Yagi, "Characterization of double-positive glutamatergic and GABAergic neurons in the gigantocellular reticular nucleus in the brainstem"第 43 回日本分子生物学会(オンライン開催), 2020 年 10 月
- [4] **Tomoki Osuka**, Hiroaki Wake, Etsuo Susaki, Katsuhiko Matsumoto, Takeshi Yagi, "Characterization of double-positive glutamatergic and GABAergic neurons in the gigantocellular reticular nucleus in the brainstem."第 45 回日本神経科学大会. 2022 年 7 月
- [5] **Tomoki Osuka**, Kazuma Furukawa, Takeshi Yagi, "Characterization of co-expression glutamatergic and GABAergic neurons in the gigantocellular reticular nucleus of the brainstem reticular formation."第 46 回日本神経科学大会. 2023 年 8 月
- [6] Hiroki Yamamoto, **Tomoki Osuka**, Takeshi Yagi, "Short-term memory abnormalities due to reduced diversity of clustered Protocadherin- α expression", 第 45 回日本神経科学大会. 2022 年 7 月
- [7] Kazuma Furukawa, **Tomoki Osuka**, Takeshi Yagi, "Importance of glutamate and GABA co-expressing neurons in SuM for recognizing of novel environment"第 45 回日本神経科学大会. 2022 年 7 月

4. Other Writings

- [8] 大須賀智輝, 「合図」を「行動」につなげる脳システムの解明 比較生理化学 37: 210-211 2020 年

5. competitive funding history

- [10]特別研究員奨励費 (DC1・生物系科学 細胞生物学関連). 大須賀智輝 (代表者). 意識形成・個体制御に関わる巨大神経網様核細胞の動態解明. 2022. 3. 8 – 2025. 3. 31